EFFECTS OF SURFACTANT ON THE MORPHOLOGY AND NIR-SHIELDING PERFORMANCE OF Cs_xWO₃ NANOPARTICLES SYNTHESIZED BY SOLVOTHERMAL METHOD

Luu Tuan Anh^{1,3*}, Tran Phuc Hoang^{1,3}, Nguyen Thi Minh Nguyet^{2,3}

¹Faculty of Materials Technology, Ho Chi Minh City University of Technology (HCMUT)

³Vietnam National University Ho Chi Minh City

ARTICLE INFO		ABSTRACT
Received: Revised: Published: KEYWORDS	27/3/2025 13/5/2025 13/5/2025	Cesium tungsten bronze (Cs _x WO ₃) is a material that exhibits excellent near-infrared shielding ability, and it has a good potential application in the energy-saving field. In this study, Cs _x WO ₃ material was synthesized by the solvothermal method, using polyvinylpyrrolidone as a surfactant to orient the structure and control the morphology of Cs _x WO ₃ particles. The change in
Cs _x WO ₃ Near-infrared Polyvinylpyrrolidone Solvothermal Surfactant		polyvinylpyrrolidone content in the reaction led to differences in the structural morphology and near-infrared radiation absorption characteristics of the material. With increasing polyvinylpyrrolidone concentration, the size of Cs_xWO_3 particles gradually decreased, the particle morphology gradually changed to a rod shape, particle aggregation decreased, and near-infrared absorption capacity was enhanced. Consequently, the surfactant polyvinylpyrrolidone plays an important role in controlling the size and structural morphology of Cs_xWO_3 particles, contributing to improving the crystallinity and near-infrared shielding ability of the material.

ẢNH HƯỞNG CỦA CHẤT HOẠT ĐỘNG BỀ MẶT ĐẾN HÌNH THÁI VÀ ĐẶC TÍNH CHE CHẮN BỨC XẠ CẬN HỒNG NGOẠI CỦA CÁC HẠT NANO $C_{s_x}WO_3$ ĐƯỢC TỔNG HỢP BẰNG PHƯƠNG PHÁP THỦY NHIỆT

Lưu Tuấn Anh 1,3* , Trần Phúc Hoàng 1,3 , Nguyễn Thị Minh Nguyệt 2,3

¹Khoa Công nghệ Vật liệu, Trường Đại học Bách Khoa - ĐHQG TPHCM (HCMUT),

của vật liệu.

THÔNG TIN BÀI BÁO TÓM TẮT Cesium tungsten bronze (Cs_xWO₃) là vật liệu có khả năng hấp thụ Ngày nhận bài: 27/3/2025 mạnh các bức xạ cận hồng ngoại và có tiềm năng ứng dụng rộng rãi Ngày hoàn thiện: 13/5/2025 trong lĩnh vực tiết kiệm năng lương. Trong nghiên cứu này, vật liệu Cs_xWO₃ được tổng hợp bằng phương pháp thủy nhiệt, sử dụng Ngày đặng: 13/5/2025 polyvinylpyrrolidone với vai trò là chất hoat đông bề mặt định hướng cấu trúc và kiểm soát hình thái hat Cs_vWO₃. Sư thay đổi hàm lượng TỪ KHÓA polyvinylpyrrolidone trong phản ứng đã dẫn đến sư khác biệt về hình Cs_vWO_3 thái cấu trúc và đặc tính hấp thu bức xa cân hồng ngoại của vật liêu. Khi tăng hàm lương PVP, các hat Cs_xWO₃ có kích thước giảm dần, Bức xa cân hồng ngoại hình thái hạt chuyển dần sang dạng thanh, sự kết tụ hạt giảm và khả Polyvinylpyrrolidone năng hấp thụ bức xạ cận hồng ngoại được tăng cường. Do đó, chất Thủy nhiệt hoat đông bề mặt polyvinylpyrrolidone đóng vai trò quan trong trong Chất hoạt động bề mặt việc kiểm soát kích thước và hình thái cấu trúc của hat Cs_xWO₃, góp phần cải thiện độ kết tinh và khả năng hấp thụ bức xạ cận hồng ngoại

DOI: https://doi.org/10.34238/tnu-jst.12404

²VNU-HCM Key Laboratory of Material Technologies, Ho Chi Minh City University of Technology (HCMUT)

²PTN Trọng điểm ĐHQG-HCM Công nghệ Vật liệu, Trường Đại học Bách Khoa - ĐHQG TPHCM (HCMUT)

³Đại học Quốc gia Thành phố Hồ Chí Minh

1. Introduction

The Sun is the most powerful, natural, and consistent radiation source, and near-infrared radiation (NIR) with wavelengths is from 780 to 2500 nm, accounting for 50% of total solar radiation energy [1]. In modern constructions, glass windows and curtain walls are frequently employed [2]. However, their lack of spectral selectivity, with a 75–90% solar transmittance, results in insufficient thermal insulation and high transmittance of NIR radiation, which is the primary cause of energy loss [3]. NIR shielding materials have received considerable attention in the applications of automotive and architectural windows due to their ability to decrease the heat from solar radiation, reduce energy consumption for air conditioning, and lower carbon dioxide emissions [4].

A variety of NIR shielding materials have been studied: rare-earth hexaborides (NdB₆, PrB₆, CeB₆, LaB₆, etc.) [5], [6], and semiconductor oxides (indium tin oxide – ITO, antimony tin oxide – ATO) [7], [8]. However, these material have their disadvantages. Cesium tungsten bronze (CWO) nanoparticle has been identified as a new contender for transparent thermal insulators because of its high visual transmittance and good near-infrared shielding capabilities. The mechanism of NIR shielding ability of CWO: small polaron and localized surface plasmon resonance is studied [9].

The synthesis methods for CWO can be categorized into two main types: solid-state reactions and solution-based methods. While specific techniques like mist chemical vapor deposition [10] and spray pyrolysis [11], [12] are highlighted, the general approaches fall into these two categories [13]. Solid-state reactions utilize dangerous hydrogen gas and high process temperatures to obtain the product of particles with microscale size. Meanwhile, the advantages of the liquid phase method, which is hydrothermal or solvothermal, are a simple synthesis process, relatively low temperature, and controllable particle size. The CWO solvothermal synthesis method has been further researched in recent years.

It has been clarified that the reducibility of solvent is very important for the solvothermal Synthesis of CWO. It has been studied that the stronger the reducibility, the more W⁵⁺ is reduced from W⁶⁺, and oxygen vacancies in CWO are created, which promotes more Cs+ cations into the hexagonal tunnels of CWO lattice [14]. Consequently, this enhances the NIR absorption of CWO. There have been many studies using organic compounds with a single hydroxyl group for solvothermal Synthesis of CWO (e.g., ethanol [15], [16], propan-2-ol [15], benzyl alcohol [17]). In some other studies, organic compounds with multiple hydroxyl groups, such as ethylene glycol and glycerol, are used as reducing agents for solvothermal Synthesis of metal oxide nanoparticles from their oxide precursors or salts [18]. However, there are no reports of organic compounds with multiple hydroxyl groups being used as reducing agents for CWO solvothermal synthesis. Using ethanol as a solvent for hydrothermal Synthesis leads to a high-pressure environment in a high-temperature environment due to the low boiling point of ethanol (78.37°C), making it difficult to control the reaction [13]. With the higher boiling point of ethylene glycol (197°C), the pressure will be lower so that the reaction is easier to control. Ethylene glycol, with its strong reducing power and relatively low cost, serves as both a solvent and a reducing agent in CWO solvothermal Synthesis.

Various attempts have been made to enhance the optical characteristics of CWO, including single- or double-ion doping and core-shell structure fabrication [19]. Additionally, the size and shape of tungsten bronze nanoparticles also affect their optical characteristics [20]. The surfactant or capping agent is an important factor in controlling nanoparticle size and morphology. The surfactant or capping agent is an important factor in controlling nanoparticle size and morphology. The surfactant is adsorbed on the surface of the CWO particles to prevent the particles from growth and agglomeration. The morphology, crystal structure, and size of the particles play important roles in CWO's NIR absorption performance and other optical-electrical properties. Several surfactants have been reported, including acetic acid [16], oleic acid [13]. Polyvinylpyrrolidone (PVP) is a non-ionic surfactant that is appropriate for investigating its effect on particles without changing the pH and charge of the solvothermal reagent system.

In this study, CWO nanoparticle is synthesized via solvothermal method using $Na_2WO_4.2H_2O$ as the W source, CsCl as the Cs source and ethylene glycol as the reducing agent and reactive solvent. Different amounts of surfactant are adjusted to investigate nanoparticle size, shape, and agglomeration. This work also studies the effect of the amount of surfactant PVP on CWO morphology.

2. Materials and methods

2.1. Materials

Sodium Tungstate Dihydrate ($Na_2WO_4.2H_2O$) and Cesium Chloride (CsCl) were purchased from Macklin. Polyvinylpyrrolidone K30 (PVP K30, MW ~ 40,000) was purchased from Sigma Aldrich (Shanghai, China). Ethylene glycol (EG), with purity of 98%, was acquired from Xilong Co., Ltd. (China). Ethanol (EtOH, purity > 99.5%) and Hydrochloric Acid (HCl, 37%) were purchased from Merck. All of the water used in the experiments was distilled water. All of the chemicals were used as received without further treatment and were of analytical grade.

2.2. Methods

Firstly, Na_2WO_4 0.25 ml/L solution was prepared by adding 0.0075 mol Na_2WO_4 in 30 ml under magnetic stirring for 15 minutes. Then, a diluted HCl solution was prepared by mixing 10 ml HCl with 50 ml DI water, and it was dropwise added into Na_2WO_4 solution under continuous magnetic stirring. When diluted HCl solution was added to the Na_2WO_4 solution, it changed from transparent to clear yellow and continued to a yellowish-white, flocculent, gel-like suspension of tungstic acid. After that, tungstic acid was redispersed in 35 ml ethylene glycol, containing different amounts of PVP (0, 0.1, 0.3, and 0.5g), by magnetic stirring until obtaining a uniform mixture. The precursor solution was prepared by mixing tungstic acid/ethylene glycol dispersion with 5 ml CsCl aqueous solution with the amount of Cs equal Cs:W = 0.33:1 ratio. Finally, the precursor solution was transferred into an 80 ml Teflon-lined autoclave and heated to 200°C in a furnace for 24 hours. After the solvothermal process, the precipitates were collected by centrifugation and washing with DI water and ethanol. The final solid was dried in a vacuum oven at 60°C for 4 hours to achieve the final product.

2.3. Characterizations

The phase composition and crystallographic structure of the CWO nanoparticles were determined by X-ray diffraction analysis (XRD, PANalytical Empyrean, England; Cu K α = 1.540598 Å). The morphology of the CWO nanoparticles was observed by scanning electron microscopy (SEM, JSM - IT200, Japan). Energy dispersive X-ray spectroscopy (EDS) was used to identify the elemental composition. The existence and quantity of PVP on the surface of the CWO nanoparticles were investigated by Fourier transform infrared spectroscopy (FTIR, NICOLET 6700 – Thermo, USA). The transmittance spectra of CWO nanoparticles dispersion were characterized by UV–Vis-NIR spectrometer (Agilent Cary 6000i, USA).

3. Results and discussion

In order to investigate the effect of various amounts of surfactant PVP on the CWO particle size and shape, precursor solution was mixed with different masses of PVP: no PVP, 0.1g, 0.3g, and 0.5g PVP, which were labeled "without PVP", 0.1PVP, 0.3PVP and 0.5PVP, respectively. All samples were synthesized under the same solvothermal process condition at 200° C for 24 hours with ethylene glycol as solvent. Figure 1 shows the diffraction peaks of samples "without PVP", 0.1PVP, 0.3PVP, and 0.5PVP, which can be indexed to the hexagonal $Cs_{0.3}WO_3$ (Ref #81-1244). While the "without PVP" sample shows no impurity peaks observed, peaks of $Cs_{1.1}W_{1.65}O_{6.5}$ phase (Ref #44-0017) appear in sample 0.1PVP. These $Cs_{1.1}W_{1.65}O_{5.5}$ peaks decrease its intensity in sample 0.3PVP and disappear in sample 0.5PVP.

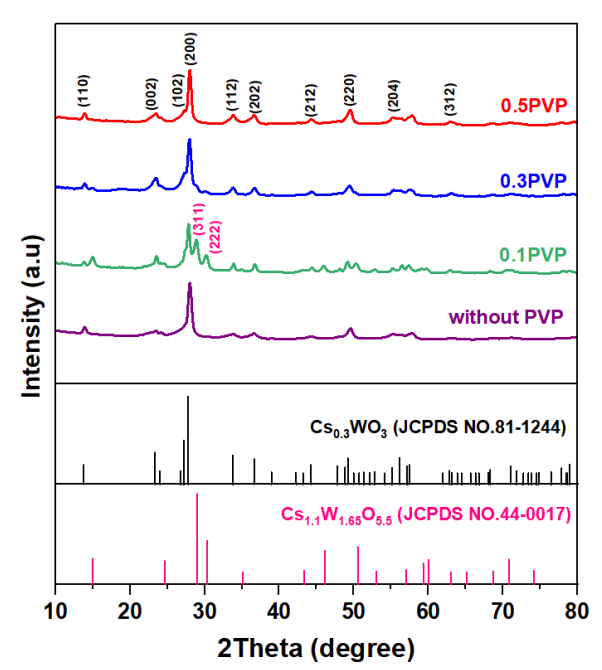


Figure 1. XRD patterns of as-synthesized Cs_xWO_3 with different amounts of PVP surfactant The crystallite size for each diffraction peak can be calculated according to the Scherrer equation (Equation 1):

$$\beta \cos \theta = \frac{K\lambda}{D} \tag{1}$$

where shape factor K is the Scherrer constant, λ is the X-ray wavelength, β is the FWHM of the diffraction peak of the crystal plane, and θ is the Bragg diffraction angle. The average crystallite size of samples is calculated (Table 1), showing that average crystallite size decreases while the amount of PVP increases. However, the average crystallite size of sample "without PVP" is smaller than sample 0.1 PVP.

Table 1. The average crystallite size of CWO nanoparticles synthesized with different PVP amounts

Sample	Average crystallite size
without PVP	17.67 nm
0.1 PVP	24.97 nm
0.3 PVP	15.2 nm
0.5 PVP	13.27 nm

Figure 2 shows the results of SEM images of the sample with different PVP content. In the SEM image of none PVP sample (Figure 2.a), irregularly agglomerated bulk CWO nanoparticles were formed. In contrast, all samples prepared with varying amounts of PVP consisted of rod-shaped particles and agglomerated particles. PVP acts to control the agglomeration of nanoparticles during the particle growth stage in the solvothermal process by selectively adhering to certain facets of the particles and attributing a steric effect. The formation of rod-shaped particles is attributed to the crystal growth of hexagonal phase CWO along the (002) crystallographic plane. The rod shape of sample 0.1PVP has the greatest length. In comparison, increasing PVP amount as sample 0.3PVP, and 0.5PVP, the length of CWO rod decreased (Table 2).

CWO synthesized with 0.1g PVP (Figure 2.b) possesses long nanorods. When increasing PVP amount to 0.3g, a decrease in the particle length can be observed in Figure 2.c. With 0.5g PVP (Figure 2.d), CWO becomes a short nanorod. Therefore, a higher amount of PVP in precursor solution leads to slower longitudinal nucleation and, hence, small growth of particles.

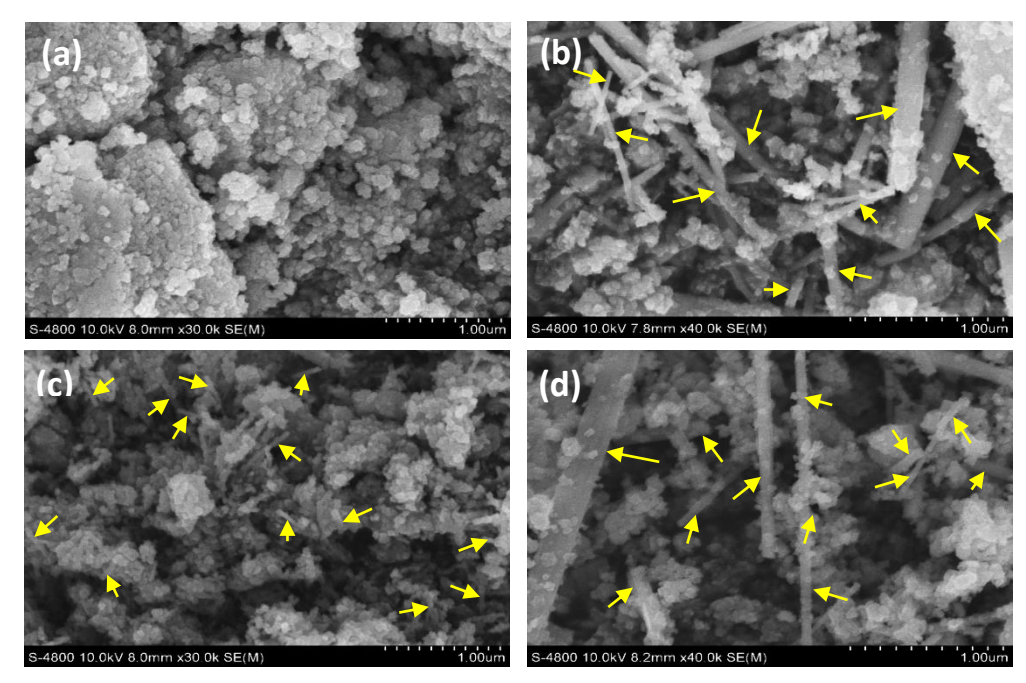


Figure 2. SEM images of CWO nanoparticles synthesized with different PVP amounts: (a) without PVP, (b) 0.1,PVP, (c) 0.3,PVP, (d) 0.5,PVP

Table 2. The average particle size of CWO rod-shaped particles synthesized with different PVP amounts

Sample	Length (nm)	Diameter (nm)
0.1 PVP	185.75	97.48
0.3 PVP	99.51	38.59
0.5 PVP	97.41	45.18

In SEM images of samples 0.1PVP, 0.3PVP, and 0.5PVP, the presence of smaller irregular particles is due to insufficient reaction time for the Ostwald ripening process to occur. Ostwald ripening involves the growth and evolution of particles in a system where nanostructured materials with large surface areas are energetically unstable due to thermodynamic factors. Nanosized particles aggregate to reduce surface energy by combining individual nanostructures. In a dispersed medium, smaller particles tend to dissolve and redeposit onto larger ones due to the differences in solubility saturation between smaller and larger particles. This diffusion process reduces the total surface energy in the system, resulting in the shrinking of smaller particles and the growth of larger particles over time. In the sample without PVP surfactant ("without PVP"), the CWO nucleation rate is faster because it is not controlled by PVP. Without the orientation provided by PVP attached to a preferred surface system (vertical direction – c axis or the outside of the rod), CWO grows uniformly in all directions. Faster nucleation also limits the growth of CWO by minimizing the number of WO₃ crystals produced that can grow on existing CWO crystals. Therefore, in the sample "without PVP", the particles do not have a certain shape.

Figure 3 illustrates the EDX patterns of CWO samples synthesized with varying PVP content. The samples predominantly contain Cs, W, and O elements, with no significant peaks indicating other elements. Table 3 presents the atomic ratios of Cs/W in different samples. In samples 0.1PVP and 0.3PVP, the presence of impurities $Cs_{1.1}W_{1.65}O_{5.5}$, with a Cs/W ratio of 1.1/1.65, results in a higher Cs/W ratio, especially pronounced in sample 0.1PVP where $Cs_{1.1}W_{1.65}O_{5.5}$ content is elevated, leading to a Cs/W ratio exceeding 0.33. As the PVP concentration increases, however, the impurity $Cs_{1.1}W_{1.65}O_{5.5}$ no longer appears in the sample 0.5PVP, and the Cs/W ratio gradually decreases, although not significantly. This decrease can be attributed to the PVP

molecules in the precursor system during the solvothermal process, which hinders Cs ions from incorporating into the WO₃ crystal lattice. The Cs/W ratio influences the near-infrared (NIR) absorption properties of the material, but other factors, such as particle size, also play a role in the NIR absorption mechanism, specifically localized surface plasmon resonance (LSPR).

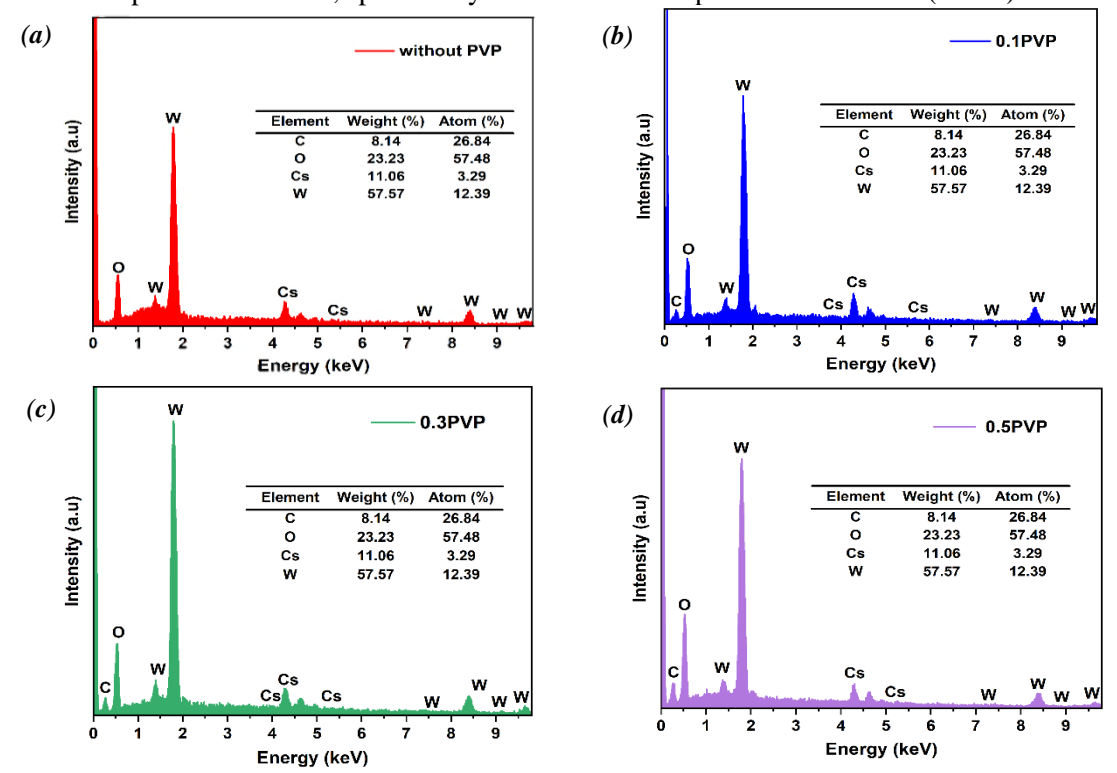
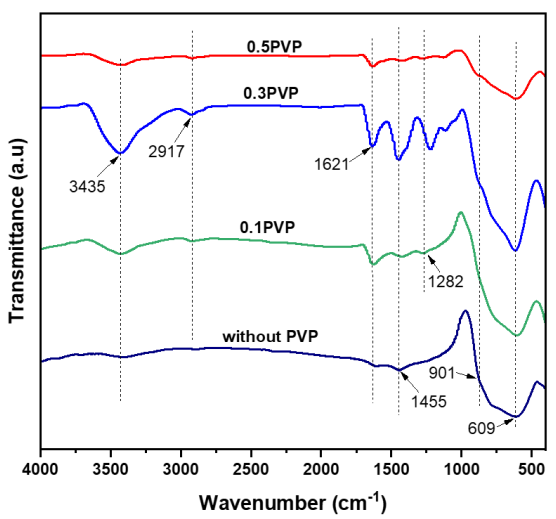


Figure 3. EDX spectrum of CWO nanoparticles synthesized with different PVP amounts: (a) without PVP (b) 0.1PVP (c) 0.3PVP and (d) 0.5PVP

Table 3. Cs/W ratio calculated from EDX spectra of CWO nanoparticles synthesized with different PVP amounts

Sample	Atomic ratio Cs/W
without PVP	0.265
0.1PVP	0.366
0.3PVP	0.269
0.5PVP	0.266

Based on the FTIR results (Figure 4), the successful coating of PVP ligands on the surface of CWO could be confirmed. The spectra of CWO containing PVP in the precursor solution exhibit characteristic absorption peaks at wavenumbers of 1282, 1455, and 1646 cm⁻¹. The peak at 1646 cm⁻¹ corresponds to the C=O stretching vibration from the lactam group in the side chains of the PVP. The peaks at 1455 and 1282 cm⁻¹ correspond to the C-N stretching vibration of the pyrrolidone ring and the N→HO complex vibrations, respectively [21]. The intensity of these three PVP peaks does not significantly change with different CWO samples. The peak at 1621 cm⁻¹ in the "without PVP" sample is related to the O-H bond attached to the W atom, and the broad peak at 3435 cm⁻¹ corresponds to the O-H stretching vibration of the -OH group on the CWO surface. This -OH group bonds with the CWO structure and cannot be simply eliminated by drying processes. The peak intensity of -OH at 3435 cm⁻¹ in the samples with PVP gradually decreases compared to the sample "without PVP" because in the absence of PVP, -OH covers the entire surface of CWO. When increasing the PVP content, PVP attached to the surface prevents -OH from attaching to the surface.



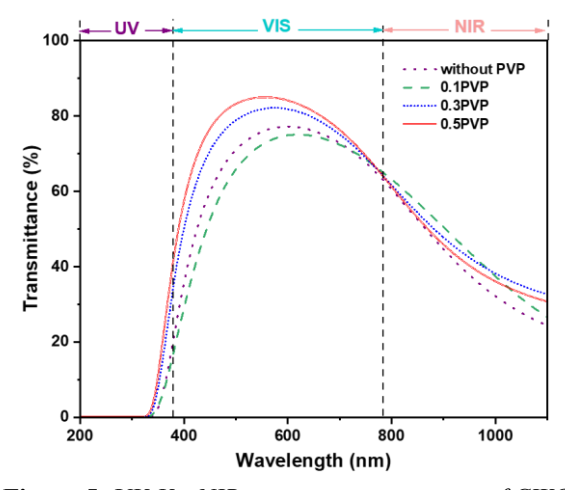


Figure 4. FTIR spectra of CWO nanoparticles synthesized with different PVP amounts

Figure 5. UV-Vis-NIR transmittance spectra of CWO nanoparticles dispersion synthesized with different PVP amounts

In CWO, specific bonds exist terminal W-O-W and bridging W-O-W. The W-O-W terminal bond is the bond between an oxygen atom and a tungsten atom in one octahedron with a tungsten atom of another octahedron, characterized on the FTIR spectrum at a wavenumber of about 901 cm⁻¹. The W-O-W bridging bond is a bond between an oxygen atom and two tungsten atoms in the same octahedron, characterized on the FTIR spectrum at a wavenumber of about 609 cm⁻¹ [22]. The decrease in both 901 and 609 peaks' intensity is because of the increase in PVP content covering WO₃ surface of CWO between different particles and the decrease of crystallite and particle size of CWO, respectively.

Figure 5 illustrates the UV-Vis-NIR transmittance spectra of different CWO aqueous dispersion samples. There is a decrease in visible transmittance with samples 0.1PVP, 0.3PVP, and 0.5PVP proportionally, while the difference in NIR transmittance is negligible. The 0.1PVP experiences a smaller slope than other samples corresponding to the contain of none NIR photothermal conversion of $Cs_{1.1}W_{1.65}O_{5.5}$ that reduces the NIR absorption of 0.1PVP sample. Based on UV-Vis-NIR transmittance measurements, the NIR-shielding ability of composite films can be quantitatively assessed using the SETS (solar energy transmittance selectivity) value, calculated according to equation (2) [23]:

SETS =
$$\frac{1}{2} \left(1 + \frac{\int_{380}^{780} E(\lambda) T(\lambda) d\lambda}{\int_{380}^{780} E(\lambda)} - \frac{\int_{780}^{2500} E(\lambda) T(\lambda) d\lambda}{\int_{780}^{2500} E(\lambda)} \right)$$
(2)

In this equation, $E(\lambda)$ is the solar irradiance spectrum. $T(\lambda)$ is the transmittance spectrum. SETS stands for solar energy transmittance selectivity, meaning the selectivity of transmitting energy through the sun. SETS values are calculated based on the solar energy transmission bias in the visible and near-infrared regions, which serves as an index to determine the NIR shielding ability of a material. A higher value indicates better NIR shielding, and a value of 0.5 indicates that the material has no NIR blocking performance. When the SETS of a film is '1', the film has 100% visible transmittance and 0% NIR transmittance. A SETS of 1 is an ideal material that can absorb all NIR radiation. The higher the SETS, the larger the deviation between T_{Vis} and T_{NIR} , which means that a sample with high SETS will have high transmittance in the visible region but low transmittance in the NIR region.

Smaller particle size means that CWO particles have a larger surface area compared to largersized CWO particles. This will increase the material's ability to absorb NIR radiation. So, the higher the PVP amount, the smaller the particle size, the lower the impurities, the better the transmittance through the visible region, and the better the NIR absorption as evidenced by the higher SETS of samples 0.1PVP, 0.3PVP, 0.5PVP proportionally (Table 4).

Sample	T _{Vis} (%)	T _{NIR} (%)	SETS				
without PVP	67.32	40.87	0.632				
0.1 PVP	64.20	45.45	0.593				
0.3 PVP	73.51	45.24	0.641				
0.5 PVP	76.56	43.52	0.665				

Table 4. SETS of CWO nanoparticles prepared with different PVP amounts

4. Conclusion

This study underscores the effective reducibility of ethylene glycol and the substantial influence of PVP surfactant content on the properties of CWO nanoparticles synthesized via a solvothermal method using ethylene glycol. The as-synthesized CWO nanoparticles exhibit excellent UV and NIR-shielding performance while maintaining high visible radiation transmittance. The results have shown that the addition of PVP surfactant has significantly affected the shape and optical property of CWO nanoparticles. 0.3g of PVP surfactant is chosen as an optinum in terms of nanorod morphology and NIR-shielding ability of CWO nanoparticles. This work advances the understanding of CWO synthesis and presents a viable approach for developing efficient NIR shielding materials for energy-efficient architectural and automotive applications.

Acknowledgements

This research is funded by Vietnam National University Ho Chi Minh City (VNU-HCM) under grant number C2024-20-15.

REFERENCES

- [1] X. Wu, J. Wang, G. Zhang, K. Katsumata, K. Yanagisawa, T. Sato, and S. Yin, "Series of MxWO3/ZnO (M = K, Rb, NH4) nanocomposites: Combination of energy saving and environmental decontamination functions," *Applied Catalysis B: Environmental*, vol. 201, pp. 128–136, 2017.
- [2] E. Cuce, S. B. Riffat, and C.-H. Young, "Thermal insulation, power generation, lighting and energy saving performance of heat insulation solar glass as a curtain wall application in Taiwan: A comparative experimental study," *Energy Conversion and Management*, vol. 96, pp. 31–38, 2015.
- [3] S. Hoffmann, E. S. Lee, and C. Clavero, "Examination of the technical potential of near-infrared switching thermochromic windows for commercial building applications," *Solar Energy Materials and Solar Cells*, vol. 123, pp. 65–80, 2014.
- [4] C.-J. Chen and D.-H. Chen, "Preparation and near-infrared photothermal conversion property of cesium tungsten oxide nanoparticles," *Nanoscale Research Letters*, vol. 8, no. 1, pp. 1-8, 2013.
- [5] H. Takeda, H. Kuno, and K. Adachi, "Solar Control Dispersions and Coatings With Rare-Earth Hexaboride Nanoparticles," *Journal of the American Ceramic Society*, vol. 91, no. 9, pp. 2897–2902, 2008.
- [6] L. Chao, L. Bao, W. Wei, and O. Tegus, "A review of recent advances in synthesis, characterization and NIR shielding property of nanocrystalline rare-earth hexaborides and tungsten bronzes," *Solar Energy*, vol. 190, pp. 10–27, 2019.
- [7] B. Shen, Y. Wang, L. Lu, and H. Yang, "Synthesis and characterization of Sb-doped SnO2 with high near-infrared shielding property for energy-efficient windows by a facile dual-titration co-precipitation method," *Ceramics International*, vol. 46, no. 11, pp. 18518–18525, 2020.
- [8] M. Kanehara, H. Koike, T. Yoshinaga, and T. Teranishi, "Indium Tin Oxide Nanoparticles with Compositionally Tunable Surface Plasmon Resonance Frequencies in the Near-IR Region," *Journal of the American Chemical Society*, vol. 131, no. 49, pp. 17736–17737, 2009.
- [9] K. Adachi and T. Asahi, "Activation of plasmons and polarons in solar control cesium tungsten bronze and reduced tungsten oxide nanoparticles," *Journal of materials research/Pratt's guide to venture capital sources*, vol. 27, no. 6, pp. 965–970, 2012.

- [10] L. Huang, H. Tang, Y. Bai, Y. Pu, L. Li, and J. Cheng, "Preparation of Monodispersed Cs_{0.33}WO₃ Nanocrystals by Mist Chemical Vapor Deposition for Near-Infrared Shielding Application," *Nanomaterials*, vol. 10, no. 11, pp. 2295-2303, 2020.
- [11] S. Nakakura, "Synthesis of Cesium Tungsten Bronze Nanoparticles by Spray Pyrolysis and Their Optical Properties," PhD. Thesis, Hiroshima University, 2020.
- [12] T. Hirano, S. Nakakura, F. G. Rinaldi, E. Tanabe, W.-N. Wang, and T. Ogi, "Synthesis of highly crystalline hexagonal cesium tungsten bronze nanoparticles by flame-assisted spray pyrolysis," *Advanced Powder Technology*, vol. 29, no. 10, pp. 2512–2520, 2018.
- [13] Y. Yao, L. Zhang, Z. Chen, C. Cao, Y. Gao, and H. Luo, "Synthesis of Cs_xWO₃ nanoparticles and their NIR shielding properties," *Ceramics International*, vol. 44, no. 12, pp. 13469–13475, 2018.
- [14] S. Ran, J. Liu, F. Shi, C. Fan, J. Yang, B. Chen, and S.-H. Liu, "Microstructure regulation of Cs_xWO₃ nanoparticles by organic acid for improved transparent thermal insulation performance," *Materials Research Bulletin*, vol. 109, pp. 273–280, 2018.
- [15] J.-X. Liu, F. Shi, X.-L. Dong, S.-H. Liu, C.-Y Fan, S. Yin, and T. Sato, "Morphology and phase controlled synthesis of CsxWO3 powders by solvothermal method and their optical properties," *Powder Technology*, vol. 270, pp. 329–336, 2014.
- [16] C. Guo, S. Yin, M. Yan, and T. Sato, "Facile synthesis of homogeneous CsxWO3 nanorods with excellent low-emissivity and NIR shielding property by a water controlled-release process," *Journal of Materials Chemistry*, vol. 21, no. 13, pp. 5099–5099, 2011.
- [17] T. Eyassu, T.-J. Hsaio, and C.-T. Lin, "Facile solvothermal synthesis of NIR absorbing Cs_xWO₃ nanorods by benzyl alcohol route," *Materials Research Express*, vol. 2, no. 1, pp. 015016–015016, 2015.
- [18] N. L. N. Broge, F. Søndergaard-Pedersen, M. Roelsgaard, X. Hassing-Hansen, and B. B. Iversen, "Mapping the redox chemistry of common solvents in solvothermal synthesis through in situ X-ray diffraction," *Nanoscale*, vol. 12, no. 15, pp. 8511–8518, 2020.
- [19] Q. Li, S. Deng, D. Li, J. Yang, H. Jin, and J. Li, "Tungsten bronze Cs_xWO₃ nanopowders doped by Ti to enhance transparent thermal insulation ability for energy saving," *Journal of Alloys and Compounds*, vol. 944, pp. 169164-169182, 2023.
- [20] L. Chao, C. Sun, J. Li, M. Sun, J. Liu, and Y. Ma, "Influence of size and shape on optical properties of cesium tungsten bronze: An experimental and theoretical approach," *Ceramics International*, vol. 48, no. 5, pp. 6436–6442, 2021.
- [21] H. U. Khan, M. Tariq, M. Shah, S. Ullah, A. R. Ahsan, A. Rahim, J. Iqbal, R. Pasricha and I. Ismail, "Designing and development of polyvinylpyrrolidone-tungsten trioxide (PVP-WO₃) nanocomposite conducting film for highly sensitive, stable, and room temperature humidity sensing," *Materials Science in Semiconductor Processing*, vol. 134, pp. 106053-106064, 2021.
- [22] V. O. Sokolov, V. G. Plotnichenko, V. V. Koltashev, and E. M. Dianov, "On the structure of tungstate—tellurite glasses," *Journal of Non-Crystalline Solids*, vol. 352, no. 52–54, pp. 5618–5632, 2006.
- [23] Y. Wang, Z. Yan, M. Zhang, Z. Zhang, T. Li, M. Chen, and W. Dong, "Flexible core–shell Cs_xWO₃-based films with high UV/NIR filtration efficiency and stability," *Nanoscale Advances*, vol. 3, no. 11, pp. 3177–3183, 2021.